

## Single-Crystal Growth of Silicon

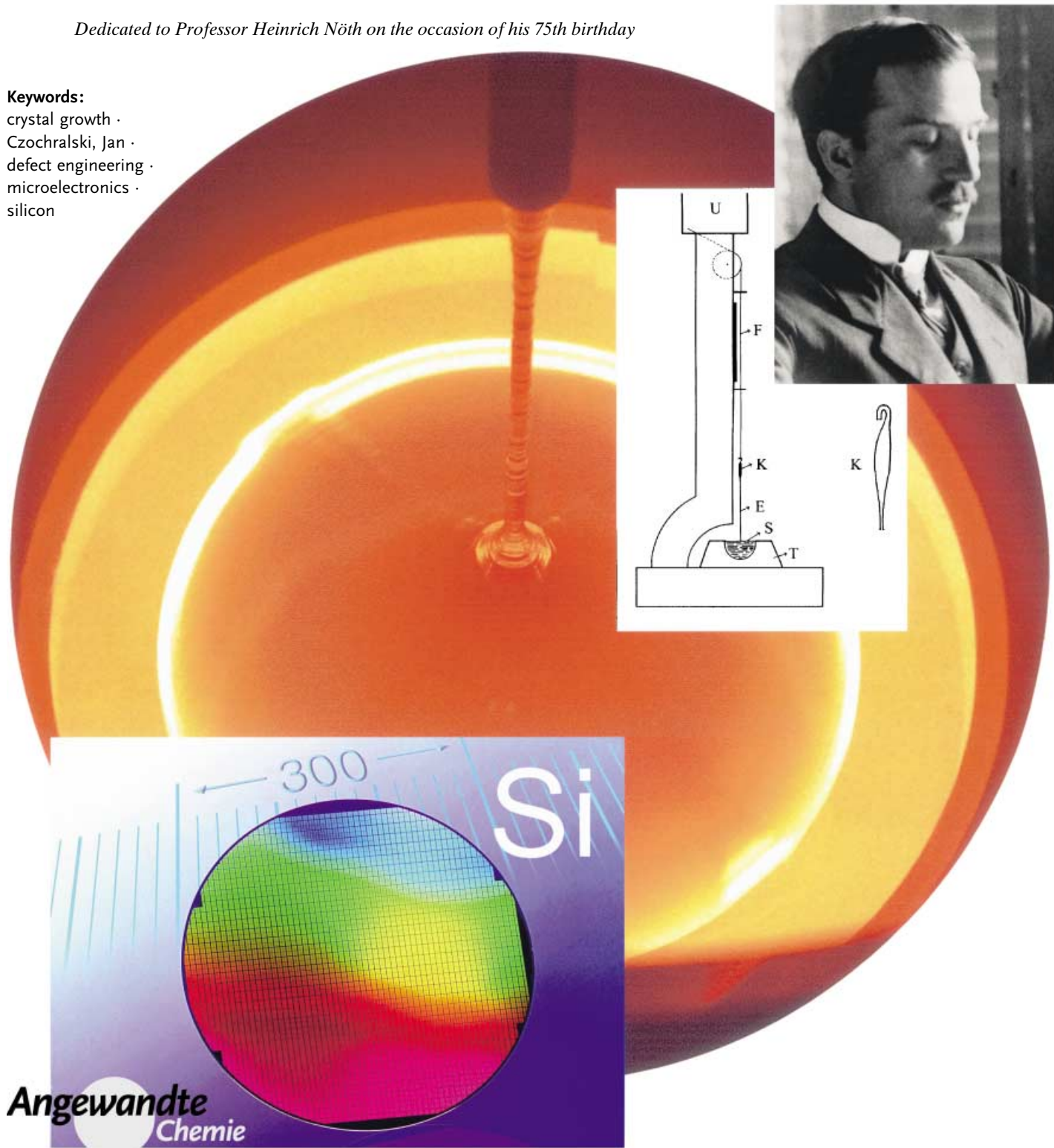
# Czochralski's Creative Mistake: A Milestone on the Way to the Gigabit Era

Jürgen Evers,\* Peter Klüfers, Rudolf Staudigl,\* and Peter Stallhofer

*Dedicated to Professor Heinrich Nöth on the occasion of his 75th birthday*

**Keywords:**

crystal growth ·  
Czochralski, Jan ·  
defect engineering ·  
microelectronics ·  
silicon



**M**uch of the rapid change in industry, science, and society is brought about by the meteoric development of the microelectronics industry. Daily life is affected by this development; one has only to think of mobile telephones and the chips on modern credit cards. The raw material for microelectronics is the single crystal of silicon, with very high purity and almost perfect crystal structure. About 95 % of the world's current production of silicon single crystals is achieved using the process that Jan Czochralski discovered in 1916. Today, single crystals of silicon can be grown that are up to 2 m long, 300 mm in diameter, and weigh up to 265 kg. The use of magnetic fields has led to significant advances in crystal-drawing technology. Intensive research and development reveals that in addition to the technology, which provides crystals of ever-increasing diameter, defect engineering, and the control of the numerous temperature-dependent reactions of crystal defects, are of paramount importance.

“...spreading understanding for technological issues...  
If we could only have travel diaries for the technical countryside that could be measured against Goethe's Italian Journey or Bismarck's Reflections and Reminiscences, the public could look at technical things with Goethe's open eyes, free them from the cold usefulness of purpose, and recognize their wonderful laws and the beauty of their existence.”

Wichard von Moellendorf<sup>[80]</sup>

## 1. Introduction

Single-crystal rods of silicon with large diameters and few defects are fundamental raw materials of the microelectronics industry that have assumed a key position in information and communication technology. The production of microelectronic components based upon silicon is a field of high technology that is under particular pressure for rapid innovation. According to the findings of G. E. Moore,<sup>[1]</sup> the capacity of electronic components (microchips) doubles in just two years with a concomitant halving in their price. Maintenance of this rapid technological advance is only possible because the line width of the incorporated electronic components is constantly reduced and consequently more functions can be accommodated on a single chip. Furthermore, with the increasing diameter of single-crystalline silicon wafers, more chips can be accommodated on a wafer and produced at the same time. It has only recently been possible to overcome this considerable cost degression per microchip through enormous technological advances. The progression from wafers of 150 mm to 200 mm diameter was achieved in 1990,<sup>[2]</sup> while the development of 300 mm wafers became possible in 1995. Since then, worldwide production of the most highly integrated chips have been produced on wafers with a diameter of 300 mm,<sup>[3]</sup> and before long the first one gigabit chips, with enough storage capacity to contain a 25-volume encyclopedia, will be available.

## From the Contents

<b>1. Introduction</b>	5685
<b>2. Jan Czochralski (1885–1953)</b>	5686
<b>3. Czochralski's Creative Mistake: Single Crystals of Tin Drawn from the Melt</b>	5688
<b>4. Preparation of Silicon Single Crystals with a Diameter of 300 mm</b>	5689
<b>5. Summary and Outlook</b>	5697

About 95 % of the world's production of silicon single crystals<sup>[4]</sup> is manufactured by the method devised by

the Pole Jan Czochralski. His method for drawing single crystals from a crucible, discovered in 1916 and described in 1918,<sup>[5]</sup> has dramatically changed daily life. Whether we communicate with a mobile telephone, pay with a chip-containing credit card in the supermarket, activate the anti-theft device in a car, or, as may soon be possible, are recognized as an individual by biometric systems, it is clear that without microchips made from single crystals of silicon, nothing would work!

In spite of this it is not an easy task to uncover anything about the life of Jan Czochralski, or the circumstances that surround his discovery. In the reading room of the Bavarian State Library in Munich it was a slow process to find out anything about the man himself. It is true that there are many references to the Czochralski method for drawing single crystals: in the Encyclopedia Britannica, the Encyclopedia Americana; in English, French, Russian, Italian, and German. However, the recent editions of reference books, sometimes comprising 20 volumes, possess no entry on Jan Czochralski himself. And in Poland? In the Wielka Encyclopedia Powszechna (12 volumes, 1962–1969), there is also no entry for Jan Czochralski. Although there is a 17-line text entry in the supplementary volume published in 1970, a search for a photograph proved unsuccessful.<sup>[6]</sup>

The first biographical data on Jan Czochralski and the quite unusual circumstances surrounding the discovery of

[\*] Prof. Dr. J. Evers, Prof. Dr. P. Klüfers  
Department Chemie  
Ludwig-Maximilians-Universität München  
Lehrbereich Anorganische Chemie  
Butenandtstrasse 5–13, 81377 München (Germany)  
Fax: (+49) 89-2180-77950  
E-mail: eve@cup.uni-muenchen.de  
Dr. R. Staudigl, Dr. P. Stallhofer  
Wacker-Chemie GmbH  
Hanns-Seidel-Platz 4, 81737 München (Germany)  
Fax: (+49) 89-6279-1466  
E-mail: Rudolf.Staudigl@wacker.com

crystal drawing were published in 1987 by P. E. Tomaszewski of the Polish Academy of Science (Wrocław) in a poorly circulated Polish-language journal.<sup>[7]</sup> Further biographical data followed two years later from J. Żmija in a report of another Polish journal,<sup>[8]</sup> and again from P. E. Tomaszewski in 1998, 2002, and 2003.<sup>[9–11]</sup>

## 2. Jan Czochralski (1885–1953)

Jan Czochralski (Figure 1) was born in Kcynia in what is now Poland on October 23, 1885 as the eighth child of an artisan family. Kcynia lies a little north of the communication link between Berlin and Warsaw, almost exactly 300 km from both cities. The region of Bydgoszcz, which contained Kcynia, was annexed by Prussia in the three Polish partitions (1772–1795), and assimilated into the German Reich in 1871. It was



**Figure 1.** Jan Czochralski, circa 1907, in Berlin.<sup>[9]</sup> (Photograph by kind permission of Dr. P. E. Tomaszewski)

only after the Treaty of Versailles that Czochralski's homeland again became Polish in 1919. Therefore, Jan Czochralski had a German upbringing. He had already become interested in chemistry while at school, but he left senior school (Teacher's Seminary in Kcynia) without graduating. At first he was only able to work on chemistry in a perfumery in Krotoszyn near his home town. This soon became too restrictive for him, and in 1904 he moved to Berlin. In an apothecary in Altglienicke owned by a pharmacist with a doctorate in chemistry he improved his knowledge of chemistry. Under expert guidance he carried out analyses of metals, ores, oils, and fats, and was found to be diligent, talented, and accurate. In 1906 he worked for a short time in the analytical laboratory of the Kunheim chemical company in Niederschöneweide near Berlin-Köpenick, and in 1907 he moved to the Allgemeine Elektrizitäts-Gesellschaft (AEG), firstly in the laboratory of the Oberspree cable works in Oberschöneweide, and then in other laboratories.<sup>[7]</sup>

In addition to his professional activities, from 1905 Czochralski attended lectures in chemistry at the technical high school in Berlin-Charlottenburg (now the Technical University of Berlin), where in 1910 he was awarded the title “Diplom-Ingenieur” for chemistry.<sup>[7]</sup> In the same year he married the Dutch pianist M. Haase.<sup>[8]</sup> He had considerable interest in music and literature, wrote poetry, and purportedly attended lectures on art and literature at Berlin University.<sup>[7,9]</sup>

From 1911 to 1914 Czochralski was assistant to Wichard von Moellendorf (Figure 2),<sup>[12]</sup> chief technologist<sup>[13]</sup> and assistant director of AEG,<sup>[14]</sup> in their metals laboratory. Von Moellendorf was an influential personality. He worked in fields stretching across science, economics, and politics; he was later undersecretary in the German Economics Ministry, was appointed Professor of National Economy, then director of the state-run Materialprüfungsamt in Berlin-Dahlem, the current Bundesanstalt für Materialforschung und -prüfung (BAM), and of the Kaiser-Wilhelm-Institut für Metallforschung. He was a member of the supervisory boards of S. Fischer Verlag, the IG Farbenindustrie, and the Metallbank und Metallurgische Gesellschaft AG (since 1928: Metall-Gesellschaft AG). From 1912 to 1916 he published a number of cultural criticisms in which he warned of the consequences of a profit-orientated economy and presented his ideas of an economic order committed to public welfare.



Jürgen Evers, born in 1941 (Dortmund), received his doctorate in 1974 with A. Weiss (LMU München) on the preparation of highly purified alkaline earths and their silicides. After postdoctoral research at ETH Zürich (1975) he gained his Habilitation in 1982 at the LMU (high-pressure investigations of silicides). He received a Heisenberg Stipendium (1985) and was appointed supernumerary professor in 1994. His research includes the study of Zintl phases at high pressure. Moreover, he is one of a rare breed who can draw a silicon single crystal by hand, albeit with 1970s technology that gives crystals of 12-mm diameter rather than 300 mm!



Rudolf Staudigl, born in 1954 (Neufahrn, Germany), received his doctorate with H. Nöth on the reaction mechanisms of boron compounds. In 1981 he joined W. N. Lipscomb (Harvard) where he worked on quantum-chemical calculations of enzyme-substrate interactions. In 1983 he moved to Wacker-Siltronic, the silicon-producing subsidiary of Wacker-Chemie GmbH, where he worked on optical fibers and GaAs crystal growth. He was president of the American subsidiary responsible for the production of high-purity silicon chips (1990–1993) and is now a company manager of Wacker-Chemie.

At AEG von Moellendorff took considerable interest in metallurgic investigations on copper and aluminum, important for electrotechnology, in which he recognized the problems of “purity and minor impurities”.<sup>[15]</sup> AEG was an innovative company that promoted research and development, and rapidly converted new scientific knowledge into technology.<sup>[12]</sup> With this research von Moellendorff awakened in his assistant Czochralski, who had until then worked essentially on analytical chemistry, an interest in metallurgy and crystallography. In 1913 a joint publication appeared on “technological conclusions from the crystallography of metals”.<sup>[16]</sup> Amongst other things, the authors showed for the first time that it was possible “by stripping from coarsely crystalline castings... to obtain individual crystals of up to the size of a finger.”<sup>[17]</sup>



**Figure 2.** The metals scientist, economic theorist, and politician Wichard von Moellendorff.<sup>[15]</sup> (Photograph by kind permission of the Bundesanstalt für Materialforschung und -prüfung).

While still a student von Moellendorff was introduced to the Rathenau family of industrialists. Since 1887 Emil Rathenau had been director general of AEG, and his son Walther (Figure 3), with a doctorate in physics, had been a member of the board of directors since 1903. After his diploma examination in 1906, von Moellendorff was employed in the AEG Oberspree cable factory. He built up a metals laboratory<sup>[14]</sup> that contained “a mechanical, a chemical, and a microscopic station” for “centralized control and research work”,<sup>[16]</sup> and he soon became chief technologist. Von Moellendorff was impressed by Walther Rathenau,<sup>[14]</sup> and a friendly relationship soon developed between the two, such that Rathenau had “great hope” in von Moellendorff.<sup>[14]</sup> In 1914 along with Rathenau, von Moellendorff encouraged the formation of the department for military raw materials<sup>[12]</sup> which was incorporated into the Ministry of War.



**Figure 3.** The scientist, industrialist, and politician Walter Rathenau, seen here as a student (circa 1890).<sup>[20]</sup> The ink well shown to the left of Rathenau has a shape consistent with that period.<sup>[21]</sup> (Photograph by kind permission of S. Fischer Verlag).

From 1914 to 1915, Rathenau was director of this new authority,<sup>[19]</sup> and he appointed von Moellendorff as one of its first co-workers.<sup>[14]</sup> With von Moellendorff's move into the “government sphere”<sup>[14]</sup> Czochralski's assistantship came to an end in 1914, and he was able to begin his own research in the metals laboratory, which he was later to lead.

From 1917 everything progressed well for Czochralski. First he moved from AEG to join the Metallbank und Metallurgische Gesellschaft AG in Frankfurt am Main, where in 1918 von Moellendorff was economic advisor<sup>[14]</sup> and, from 1919, a member of the supervisory board.<sup>[12]</sup> There, as head of the metals laboratory, Czochralski combined excellent research with economic awareness. With a number of scientific colleagues he founded the German Society for Metals Science in 1919, of which he was president from 1925 until his appointment as professor at the chemical faculty of the Technical University in Warsaw in 1929. After a short period he founded a department for metallurgy and metals science at the university. He even acquired his own research institute, a very rapid ascent for an artisan's son who failed to graduate from high school. His successful work in industry and science in his country of birth brought him high recognition in his homeland. But the Second World War brought about Jan Czochralski's downfall.

The German invasion of Poland in 1939 and the effects of the war eventually led to the complete cessation of his research in Warsaw. At the request of his co-workers he founded a workshop in the institute that produced replacement parts for both the German and Polish self-administration in occupied Warsaw. For those living under duress, that not only brought a means of existence, but also, since official documentation was issued, protection from the random incursions of occupying forces. Czochralski actively supported the Polish underground army and helped many of those in need in the Warsaw ghetto, but after the war the senate of the Technical University of Warsaw accused him of collaboration with the Germans, and in 1945 excluded him from the university.<sup>[7,9]</sup>

Embittered, he returned to his home town of Kcynia, and using his acquired knowledge of pharmacy and perfumery

founded BION, a small company for cosmetics and household chemicals in 1946. He died in Poznań on April 22, 1953 at the age of 68 and was buried in Kcynia.<sup>[7,9]</sup> The tragedy of his ever-active life was publicized in 2001 by the fact that in the list of unclaimed Swiss bank accounts with assets deposited before or during the Second World War, there is an entry for a “Czochralski, Jan [Poland]”.<sup>[22]</sup> However, Swiss banks give detailed information only to persons with a valid claim.

The bond between Walther Rathenau, Wichard von Moellendorff, and Jan Czochralski is typified by the manner their lives were thwarted by the tragic circumstances of the age: Rathenau, appointed German Foreign Minister in 1922, was shot by two young radical right-wing officers in June of the same year.<sup>[19]</sup> Von Moellendorff killed himself four years after the seizure of power by the National Socialist Party and the suicide of his Jewish second wife.<sup>[12]</sup>

Jan Czochralski's first publication, in 1913 with Wichard von Moellendorff at AEG, dealt with technological aspects of the crystallography of metals.<sup>[17]</sup> His final publication appeared in 1940 in the Swiss Archive for Applied Science and Technology and dealt with the results of some basic research on aluminum.<sup>[23]</sup> At that time the first European aluminum facility in Neuhausen am Rheinfall (Switzerland), in which Walther Rathenau once worked as technical appointee, was only 50 years old. In 27 years Czochralski published 101 metallurgic publications,<sup>[7]</sup> of which 70 are referenced in Chemical Abstracts. These include a text book (Modern Metal Science in Theory and Practice), which was published by Julius Springer in 1924 and which was later translated into several languages.<sup>[24]</sup>

After his exclusion from the Warsaw Technical University, Jan Czochralski sank into obscurity under the communist regime. He found greater recognition only after his death. Seventy years after the discovery of crystal drawing, the 10th European Crystallographic Meeting in Wrocław (1986) was dedicated to his memory.<sup>[7]</sup> Today, Jan Czochralski is recognized as one of the most highly regarded Polish natural scientists (a list of 14 outstanding natural scientists born in Poland was published by the Polish Physical Society<sup>[25]</sup>). Jan Czochralski stands alongside Maria Skłodowska-Curie, Walther Nernst, Otto Stern, and Albert Michelson. On the occasion of the 50th anniversary of Czochralski's death the Polish Society for Crystal Growth held an international symposium in Toruń and Kcynia at the end of April 2003.<sup>[26]</sup>

### 3. Czochralski's Creative Mistake: Single Crystals of Tin Drawn from the Melt

The famous discovery, the effects of which can be felt today, was made by Czochralski at AEG in Berlin.<sup>[5]</sup> He submitted a paper to *Zeitschrift für Physikalische Chemie* in August 1916, which appeared in the February issue of 1917, but was only classified for the first time in Volume 92 in 1918. He had also communicated his results briefly to the *Zeitschrift des Vereines Deutscher Ingenieure* in April 1917.<sup>[27]</sup> In retrospect, it is surprising to note that Czochralski made this fundamental discovery through a creative mistake!

According to the research of P.E. Tomaszewski,<sup>[7,9–11]</sup> Czochralski was working on the rate of crystallization of metals and one evening had terminated an unsuccessful experiment with a tin melt. He carefully placed the full, hot crucible on the edge of the desk to cool. He then began to enter notes into the laboratory notebook. The necessary utensils of the time (pen and ink well) were on the desk. Then, as Czochralski confirmed nine years later, a “remarkable coincidence” took place.<sup>[18]</sup> He was totally fixated on the notes, and deep in thought he dipped his pen not into the ink well, but into the crucible with molten tin.<sup>[7,9–11]</sup> Alarmed, he quickly lifted his arm and noted that a long, thin thread was hanging onto the pen. It was, through etching with acid, to be the first single crystal drawn out of a crucible by the Czochralski method! A single crystal of tin had separated from the liquid tin due to the capillary-like constriction of the tip of the steel pen on its removal. This thin single crystal acted as a seed to which further tin atoms from the melt attached themselves to the single crystal.

Figure 4 illustrates the apparatus of 1916, unpretentious by modern standards, with which Jan Czochralski made his discovery reproducible “with ease” as he himself later put it.<sup>[24]</sup> With this apparatus he prepared single crystals of tin, lead, and zinc. The length of the single crystals of tin drawn in the first Czochralski apparatus was about 15 cm with a diameter of about 1 mm and a mass of about 1 g.

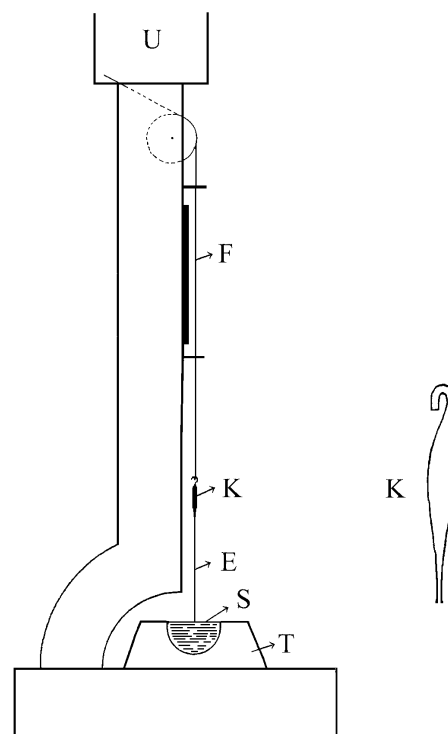


**Figure 4.** Czochralski's crystal drawing apparatus of 1916.<sup>[5]</sup> The clockwork motor (U) draws the single crystal (E) out of the melt (S) which sits in the crucible (T). The seed crystal resides in a capillary (K), which is attached to a thread (F). The capillary (K) is shown on the right-hand side of the apparatus, magnified six times. From a diagram by J. Czochralski.<sup>[5]</sup>



#### 4. Preparation of Silicon Single Crystals with a Diameter of 300 mm

##### 4.1. A Backward Glance

As previously stated, about 95 % of the world's production of silicon single crystals is manufactured by the Czochralski (CZ) procedure.<sup>[4]</sup> It is interesting to note how rapidly the diameter of silicon single crystals has increased over the last three decades. At the beginning of the 1970s one of the authors (J.E.) had prepared crystals of 12 mm diameter on a hand-operated drawing apparatus (Siemens VZA 3) at the Inorganic Chemistry Institute of the Ludwig Maximilian University in Munich. At that time, industrial technology was already at 50 mm. In 1980 this had reached 100 mm, then 200 mm by 1995, and by 2002 the technology was at a diameter of 300 mm. Wacker-Chemie GmbH (Burghausen, Germany) supplies 300-mm diameter wafers (the only supplier of such wafers outside of Japan) on which the chips are produced at Infineon Technology AG (Dresden, Germany).<sup>[28]</sup> The Shin-Etsu group and the company Sumco are involved in manufacture of wafers in Japan.

##### 4.2. Industrial Growth of Silicon Single Crystals with a Diameter of 300 mm

Figure 5 displays a cooled silicon single crystal with a diameter of 300 mm, about 2 m in length, and weighing approximately 265 kg that was produced by the CZ method. At the top of the single crystal is situated the thin seed which at the start of drawing is dipped into a crucible containing molten silicon and then, as with Jan Czochralski in 1916, pulled out again, but in this case very slowly.

Figure 6 schematically illustrates a CZ drawing plant in which such silicon single crystals of 300-mm diameter are produced.<sup>[29]</sup> The total height is about 15 m, hence the upper part of the drawing mechanism is shown in a somewhat truncated form.

The silica crucible (4) from which the single crystal (3) is drawn from the melt (1) on a seed (2) at about 1420 °C is supported by a graphite crucible (5) because silica softens at these temperatures. The SiO<sub>2</sub> crucible and the Si single crystal may be rotated and each is adjustable upwards or downwards. External magnetic coils (7) can be attached at the furnace chamber so that the single crystal may also be drawn from the melt under the influence of a magnetic field. The furnace chamber may be sealed under high vacuum, but during the growth period it is filled with argon as protective gas. The growth process may be monitored and controlled directly with an optical sensor (13).

Six steps in the CZ growth of a silicon single crystal are illustrated in Figure 7. After evacuating to 10<sup>−3</sup> mbar, polycrystalline pieces of highest-purity silicon are heated to a temperature just above the melting point of silicon (1414 °C) under a pressure of 10–200 mbar of high-purity argon (Figure 7a).<sup>[30,31]</sup> When thermal equilibrium has been reached in the melt (Figure 7b) the thin Si seed crystal (3–5 mm in diameter) with the desired crystallographic orientation (in



**Figure 5.** A single crystal of silicon, 300 mm in diameter, 2 m long, and weighing 265 kg, drawn using the CZ process. (Photograph: Wacker-Chemie).

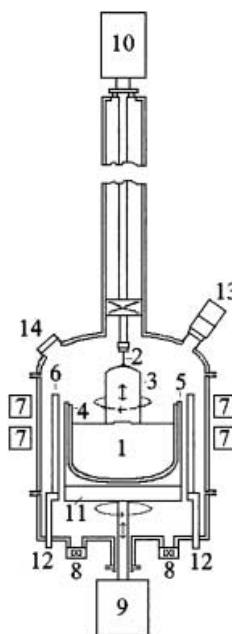


**Figure 6.** Diagram of a CZ drawing plant for 300-mm diameter silicon single crystals. The total height of the drawing plant is about 15 m, therefore the upper section of the installation is somewhat truncated (diagram after B. Altenkrüger and M. Gier).<sup>[29]</sup> 1 melt, 2 seed, 3 single crystal, 4 silica crucible, 5 graphite crucible, 6 heating elements, 7 magnetic coils, 8 argon outlet, 9 rotating equipment for the crucible, 10 drawing and rotating equipment for the crystal, 11 crucible mounting, 12 current supply for the heating elements, 13 optical sensor, 14 viewing glass.

almost all cases [100]) is dipped into the melt (Figure 7c). Slight cooling induces crystallization at the Si seed as a thin neck ("necking"; Figure 7d). With a rapid rate of crystalliza-

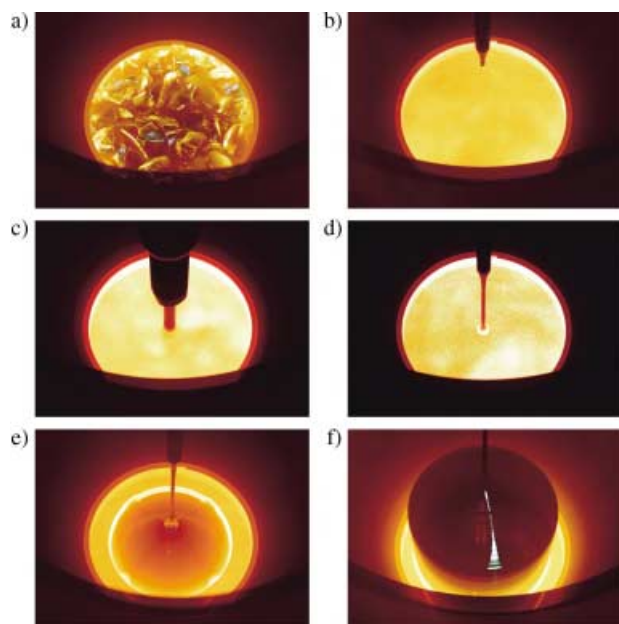


**Figure 7.** Six steps in the CZ growth of a silicon single crystal: a) Evacuation and heating of the polycrystalline silicon ("pumping"); b) setting the temperature of the Si melt just above 1414 °C ("melting"); c) dipping the thin Si seed crystal into the homogeneous Si melt ("dipping"); d) initiating crystallization at the neck of the thin Si seed ("necking"); e) adjustment of the shoulder of the desired single crystal diameter ("shoulder"; four positions which portray the fourfold drawing axis [100] are visible at the hot, light marginal zone of the single crystal); f) growing phase of the single crystal with constant diameter ("body"). (Photographs: Wacker-Chemie)

tion, drawing is then carried out at a rate of a few millimeters per minute. Because of the high growth rate, one-dimensional crystal defects (dislocations) can no longer spread because their diffusion-controlled growth in the [100] direction no longer keeps pace. They grow laterally and end up at the surface of the thin necks. (The migration of dislocations will be discussed in more detail in Section 4.6.). In this way dislocation-free silicon ("DF-Si") is formed after a few centimeters of growth.<sup>[32]</sup> By further reduction in temperature the diameter is increased. Finally, at the desired diameter, the growth in thickness is slowed down and the crystal is "bent over" ("shoulder"; Figure 7e). Four points are visible at the hot, bright marginal zone of the single crystal which form an image of the fourfold drawing axis [100]. The main process, namely, the drawing of the Si crystal from the melt with constant diameter, then begins. For the 300-mm single crystal shown in Figure 5, a total time of 3–4.5 days is needed for a crystal length of 2 m. The drawing rate in the cylindrical part is 0.4–1.2 mm min<sup>-1</sup>, depending on the desired crystal properties and the intended use. The process parameters must be continuously adjusted during drawing because the mass of the Si melt of 300 kg at the start falls to 35 kg towards the end of the process. B. Altekruiger and M. Gier have detailed the technology of CZ drawing of 300-mm silicon single crystals.<sup>[29]</sup>

The transition from the 200-mm to the 300-mm technology was a considerable technological advance.<sup>[33]</sup> Above all, with this increase in diameter, the amount of polycrystalline silicon had to be increased from 110 kg to about 300 kg, which

necessitated an enlargement of the diameter of the silica crucible from 60 to 80 cm. The tripling of the silicon charge for crystal growth also required reconstruction of the drawing apparatus. To maintain the previous demands for axial accuracy of the drawing plant and to exclude any oscillation during crystal growth, the drawing plant was equipped with three-column, rather than single-column hydraulics.<sup>[34]</sup> Figure 8 shows the CZ crystal-drawing apparatus EKZ 3000/400 of CGS-Crystal Growth Systems GmbH (Hanau, Germany) for crucible diameters of up to 102 cm and a maximum Si melt of 600 kg.<sup>[35]</sup>



**Figure 8.** CZ crystal drawing apparatus for crucible diameters of up to 102 cm and a maximum of 600 kg silicon melt.<sup>[35]</sup> (Photograph with kind permission of Crystal Growing Systems GmbH).

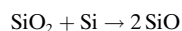
### 4.3. Technical Problems

Two serious problems occurred during the growth of 300-mm single crystals from crucibles with up to 300 kg silicon melt. First, as a result of the long processing time, the high load demanded an extremely clean and bubble-free silica crucible. In addition, the heat balance and thus the temperature distribution in the Si melt had to be precisely controlled because turbulent flows occurred in the total melt volume. These factors greatly impaired single-crystal drawing and made it difficult to achieve a homogeneous temperature distribution in the crystal during cooling because of the large crystal diameters and masses.

The maximum drawing rates are reduced in comparison to the 200-mm crystals, since latent heat ( $1.8 \times 10^6 \text{ J kg}^{-1}$ )<sup>[36]</sup> is released during crystallization (enthalpy of crystallization,  $\Delta H = -50.21 \text{ kJ mol}^{-1}$ ).<sup>[37]</sup> This heat at the crystallization interface of silicon single crystals of 300-mm diameter is, with respect to surface area, 2.25 times greater than for those

of 200-mm diameter. This heat, which arises in the center of the crucible, must be dispersed. In addition, the temperature of the melt at the crystal/melt boundary must be cooler so that the crystal grows truly. Moreover, the axial temperature gradient across the crystal is changed.<sup>[33]</sup>

The reduced drawing rate for 300-mm single crystals and the increased weight leads to a doubling of the time in which the crucible material ( $\text{SiO}_2$ ) is in contact with the Si melt. This can cause corrosion phenomena, and in extreme cases, to the release of  $\text{SiO}_2$  particles into the Si melt, which can lead to dislocations in the Si crystal. However, the reaction of silica with liquid silicon<sup>[38]</sup> leads to desired doping of the melt with oxygen [Eq. (1)].



Oxygen is transported in part by convection and diffusion to the free melt-gas surface where it evaporates as  $\text{SiO}$  and is blown off with high-purity argon and pumped away. Some of the oxygen dissolved in the melt is transported to the melt-crystal phase boundary and incorporated into the crystal lattice, which leads to oxygen doping of the crystal and wafer. An oxygen doping  $N_{\text{O}}$  of  $4 \times 10^{17}$  to  $\approx 7 \times 10^{17}$  O atoms per  $\text{cm}^3$  (hereafter given as  $N_{\text{O}}$  [ $\text{cm}^{-3}$ ]) is desired depending upon the application and process methodology used during chip manufacture. In the case of silicon, which has a density of  $2.329 \text{ g cm}^{-3}$  and a molar mass of  $28.08553 \text{ g mol}^{-1}$ ,<sup>[37]</sup> an  $N_{\text{O}}$  value of  $5 \times 10^{17} \text{ cm}^{-3}$ <sup>[38]</sup> corresponds to  $5 \times 10^{22}$  Si atoms per  $\text{cm}^3$  (or 0.001 at%), and to 10 ppma O (ppma = atoms per million). To be able to maintain such oxygen doping it is necessary that 99% of the oxygen that is carried into the Si melt through crucible corrosion diffuses to the free melt-gas interface and is removed as  $\text{SiO}$ . Only the residue of about 1% of the oxygen may be incorporated into the single crystal,<sup>[38,39]</sup> but this amount must be maintained very accurately.

#### 4.4. The Magnetic Czochralski Procedure (MCZ)

The high demands placed upon oxygen control in the large melt volumes, crucible surfaces, and the changed ratio of free-melt surface to crystal diameter could no longer be totally fulfilled by conventional CZ growth. In addition, for certain process conditions there were problems in governing precise temperature control over three times the melt volume, relative to that used to prepare 200-mm technology. The temperature stability required for good single-crystal quality cannot always be guaranteed with mechanical rotation alone (e.g., 5 rotations  $\text{min}^{-1}$  for the crucible in one direction and 15 rotations  $\text{min}^{-1}$  in the opposite direction for the single crystal); at high melt volumes convection is unstable, which corresponds to turbulent flow.

A turbulent flow in the melt can be suppressed more effectively through electromagnetic forces<sup>[40]</sup> than with mechanically produced forces, or can be actively driven using dynamic magnetic fields; this process is known as the magnetic CZ procedure (MCZ). Unlike crystalline silicon at room temperature, liquid silicon is a good conductor of electricity. According to the fundamental electrodynamic laws,<sup>[41]</sup> Lorentz forces are exerted by a static magnetic field (a “cusp” or horizontal magnetic field) on moving charges that are perpendicular to the magnetic-field vector and the rate vector, in the sense of a right-handed helix. The Lorentz forces in the Si melt are greatest when an orthogonal arrangement of both vectors exists.

Three possible arrangements of the magnetic coils in the MCZ procedure are shown in Figure 9, and are the state of the art for static fields: The magnetic field can be produced

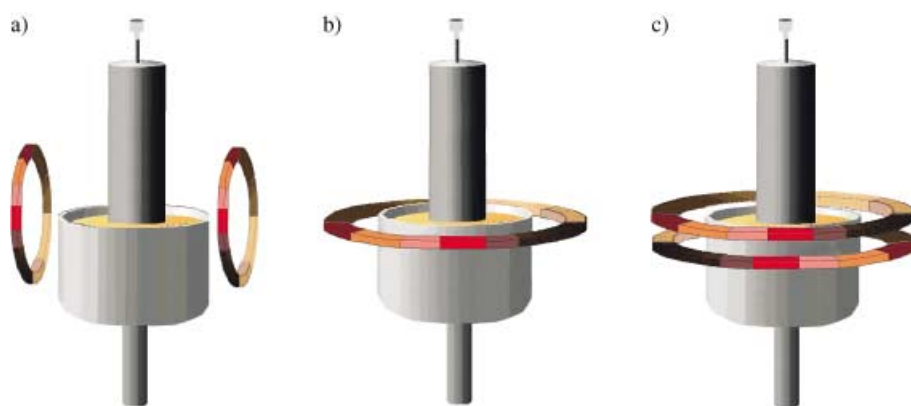


**Figure 9.** Arrangement of the magnetic coils for the magnetic CZ process with static fields: a) Horizontal, b) axial, c) cusp magnetic fields. To produce the cusp magnetic field the currents must flow in opposite directions in the two coils.

transversally through two horizontal toroids (HMCZ; Figure 9a). The magnetic field lines run perpendicular to the drawing direction of the crystal. In the second variant (Figure 9b) the toroid is arranged vertically and produces an axial magnetic field, while in the third arrangement (Figure 9c) two coaxial toroids, in which the electric currents flow in opposite directions, are arranged symmetrically about the melt-crystal interface to produce a cusp magnetic field (the word “cusp” is derived from the Latin *cuspidis* = point, lance.<sup>[42]</sup> The points in the tracery of a gothic church window are known as “cusps”.<sup>[43,44]</sup>) The opposed toroids produce the cusp magnetic field, which leads to zero magnetic-field strength at the center of the melt-crystal interface. However, the magnetic-field strength increases rapidly in all other directions.

Systematic investigations in MCZ plants have shown that oxygen transport through convection is reduced and thus lower oxygen concentrations can be regulated using cusp magnetic fields.<sup>[39]</sup> In addition, turbulent fluctuations are suppressed.<sup>[45]</sup> Fields of up to 3000 G can be produced at the rim of the crucible with superconducting magnets that produce cusp-geometry fields, in which the field at the



growth boundary is practically zero.<sup>[46]</sup> Horizontal fields also make these high fields possible at the crystal.

A new technology (developed by Wacker) is the dynamic magnetic field (“traveling magnetic field”, or the combination of a cusp field with alternating current fields), which actively imposes the desired convection pattern and thus allows far more possibilities for influencing the melt than passive, static fields can offer. The convection pattern can be set according to the direction of the traveling magnetic fields. This can be advantageous with respect to stabilization of growth and oxygen control, since convection affects both heat and oxygen transport. In addition, significantly less power and space are required for dynamic fields, which offers advantages in respect of the demands for lower production costs. Figure 10 illustrates a MCZ arrangement in which dynamic fields are employed.

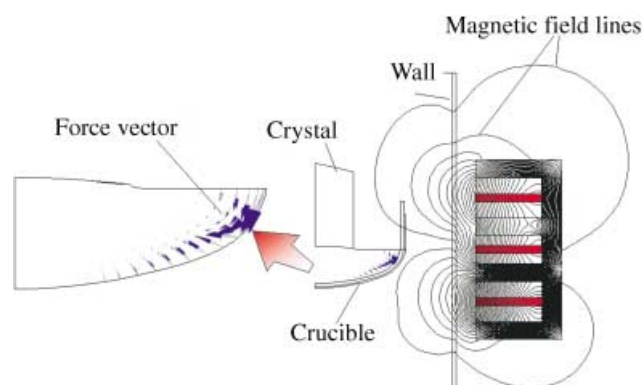


**Figure 10.** Dynamic fields (traveling magnetic fields) in the magnetic CZ process. On the right the arrangement of the coils and the resulting magnetic field lines are illustrated schematically. On the left the resulting forces on the melt are shown. By changing the direction of the traveling field the direction of force, and thus the flow of the melt, can be reversed.

The active driving of the melt using traveling magnetic fields is based on the same principle that applies in linear motors, for example, in transport through magnetic levitation, such as with the Transrapid train. When the magnetic field is at a maximum, the alternating field induces a current at a certain point that interacts with the traveling magnetic field and thus drives the melt.

#### 4.5. Mathematical Modeling of Crystal Drawing

Recently it has become possible to mathematically simulate oxygen diffusion and temperature distribution in a silicon melt in the silica crucible of a MCZ plant with cusp magnetic fields.<sup>[39]</sup> Figure 11 shows schematically the model for calculating<sup>[39]</sup> the number of oxygen atoms  $N_O$  at three positions: in the Si melt at point M and in the Si single crystal at points S and Z, which is viewed both from the side (Figure 11, top) and from above (Figure 11, bottom).

The coils producing the cusp magnetic fields (1 and 2) are aligned parallel to the melt–crystal interface (Figure 11, top;

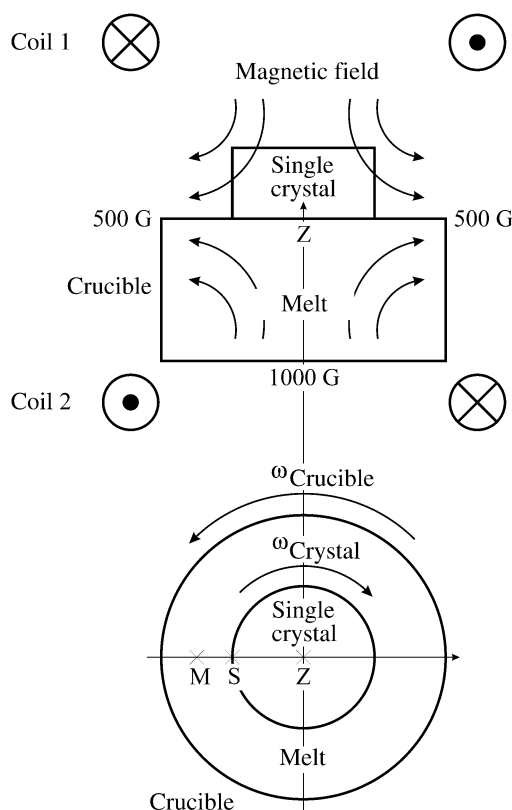


**Figure 11.** Model for the calculation of the oxygen concentration in the silicon melt and in the silicon single crystal of a MCZ arrangement with a static cusp magnetic field. Top: side view, bottom: plan view.<sup>[39,47]</sup>

the symbols  $\otimes$  and  $\odot$  represent the opposite directions of the current within the two coils that produce the cusp magnetic field). The path of the field lines of the cusp magnets is also shown. At the base of the silica crucible the magnetic field has a strength of 1000 G, while at the upper rim both sides of the crucible it is 500 G. The center (point Z) of the melt–crystal interface is magnetic-field free. Owing to the considerable computational expenditure of the model, the single crystal is calculated to be only 37.5 mm in diameter (i.e., 1/8 of the real diameter). Correspondingly, the crucible, with a diameter of 75 mm, is considerably smaller than that which is used in 300-mm technology. The crucible and crystal are rotated in opposing directions. In the plan view (Figure 11, bottom) two further points for oxygen calculation are shown: point M is located between the crucible rim and the crystal surface, and point S is at the crystal surface. The magnetic field is entered into the calculation as the dimensionless Hartmann number  $Ha$ ,<sup>[47,48]</sup> which in magnetohydrodynamics describes the flow field of an electrically conducting liquid in a magnetic field.

Figure 12 shows the concentration of oxygen atoms  $N_O$  as a function of time  $t$  in the melt at points M, S, and Z.<sup>[39,47]</sup> On the left side of the chart, the cusp magnetic field ( $Ha = 161$ ) is switched on, and on the right side it is switched off ( $Ha = 0$ ). Between  $t = 400$  and  $t = 600$  s,  $N_O \approx 1.3 \times 10^{18} \text{ cm}^{-3}$  at point M (Figure 12). During this time period, the plot for point M shows sharp periodic signals, which clearly demonstrates that the cusp magnetic field suppresses turbulent aperiodic

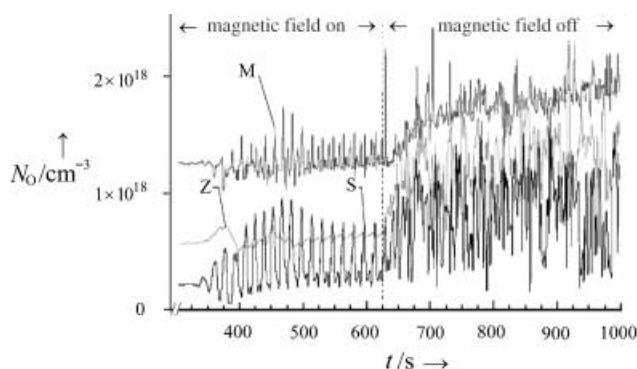


**Figure 12.** Number of oxygen atoms  $N_O$  [ $\text{cm}^{-3}$ ] as a function of time  $t$  with and without static cusp magnetic field in the melt (M), on the crystal surface (S), and in the center of the melt–crystal interface (Z). Data from Ref. [39]; see text for more details and Ref. [47].

fluctuations.<sup>[45]</sup> The periodic oscillations are caused by convective instabilities<sup>[49]</sup> when dominant vertical temperature gradients occur in rotating liquids.<sup>[50]</sup> With the cusp magnetic field switched off ( $Ha=0$ ), the oscillations lose their periodicity in the model described. If a weak cusp magnetic field is applied, as observed at point Z (Figure 11, top), the periodic signals at that point are correspondingly weak (Figure 12).

Switching off the magnetic field at  $t=625$  s results in an increase in  $N_O$  to  $1.8 \times 10^{18} \text{ cm}^{-3}$  at point M. Thus, more oxygen atoms are carried into the melt at M. At the same time intense aperiodic fluctuations in the oxygen concentration occur. With the cusp magnetic field switched on, the  $N_O$  values are about  $0.3 \times 10^{18}$  for S,  $0.6 \times 10^{18}$  for Z, and  $1.3 \times 10^{18} \text{ cm}^{-3}$  for M. Switching off the magnetic field also causes an increase in oxygen concentration at points Z and S. With the cusp magnetic field applied, the value of  $N_O$  at Z ( $\approx 0.6 \times 10^{18} \text{ cm}^{-3}$ ) and S ( $\approx 0.3 \times 10^{18} \text{ cm}^{-3}$ ) is only one third and one sixth, respectively, of that at point M when no magnetic field is applied ( $\approx 1.8 \times 10^{18} \text{ cm}^{-3}$ ). Switching on the cusp magnetic field thus brings about a purifying effect with regard to the concentration of oxygen impurities in CZ silicon.

A cusp magnetic field also has a favorable effect on temperature distribution in the Si melt and at the boundary zone of a CZ-grown Si single crystal.<sup>[45]</sup> For calculations of these effects, a model with a smaller silica crucible (107 mm high with a diameter of 360 mm) and crystal diameter (104 mm) was required. The cusp magnetic field was set at a maximum of 400 G. The whole melt and the lower part of the single crystal were broken down into a matrix of 450 000 control volumes to calculate the temperature distribution. Figure 13 illustrates the measured and calculated normalized temperature distribution (isothermal lines) in the melt of a MCZ plant with the cusp magnetic field switched off (Figure 13a) and switched on (Figure 13b).<sup>[45,51]</sup>

The left side of Figure 13a shows the temperature measured in the crucible of a 20-kg CZ silicon melt without magnetic field, and the right side shows the equivalent

calculated temperature. Figure 13b shows the same information with an applied cusp magnetic field of 400 G. The maximum temperature difference measured ( $\Delta T_{\text{max}}$ ) is  $36^\circ\text{C}$  with no applied field, and  $42^\circ\text{C}$  with the cusp magnetic field switched on.<sup>[45]</sup> By this method, direct temperatures may again be calculated from the normalized isothermal lines at a known silicon melt temperature, which allows greater insight into the temperature distribution within the crystal.<sup>[51]</sup>

The agreement between experiment and simulation is very good: The difference between measured and calculated temperature is no more than  $4^\circ\text{C}$  without field, and  $6^\circ\text{C}$  with the magnetic field switched on.<sup>[45]</sup> Figure 13b shows that a considerable dampening of convective heat transport and a greater temperature difference between crystal and crucible rim is achieved with the magnetic field switched on. This is exemplified by comparison of, for example, the experimental

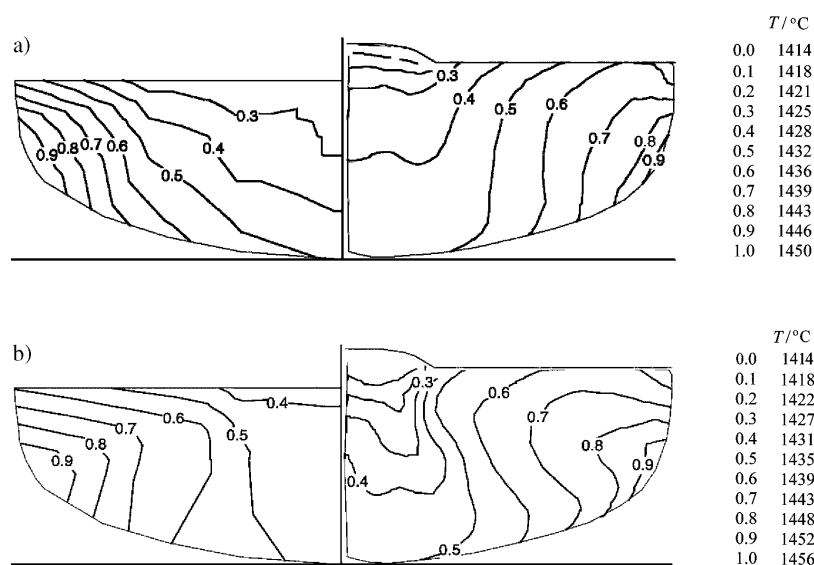


**Figure 13.** Normalized temperature distribution of a 20-kg silicon CZ melt; <sup>[45]</sup> left: measured, right: calculated for a) without field, and b) with a cusp magnetic field of 400 G. See text and Ref. [51] for details.

isotherms 0.6 on the left-hand side of Figure 13a and b: The isotherms run almost perpendicularly; there is less heat exchange through convection in a radial direction since the cusp field inhibits melt movement in a radial direction at the crucible rim (that is, perpendicular to the magnetic field lines).

Mathematical modeling of crystal-growth processes is also a useful tool for simulating changes in furnace construction and thus the optimization of cooling rates and defect kinetics. Corrosion of the silica crucible by the Si melt at different process parameters may also be estimated in this way. Costs are reduced dramatically if expensive experimental investigations can be simulated by a click of a mouse. Thus computer programs, for example, CrysVUN++<sup>[52]</sup> or FEMAG-CZ,<sup>[53]</sup> are of considerable economic significance when it comes to increasing the diameters of silicon single crystals beyond 300 mm.

#### 4.6. Defects in Silicon Single Crystals

A manufactured crystal of silicon with a diameter of 300 mm is very different from the fictional ideal crystal with a three-dimensionally extended translational periodic structure; a multitude of deviations from the perfect crystal arise. These defects can be produced by silicon itself, or by impurities. Since these defects are mobile at elevated temperatures they react with each other in many ways during the cooling phase of the large single crystal, which takes several days. In addition to the desired reactions, undesired processes can take place whose consequential products can produce fatal defects in the active switching region of the microchip and cause considerable economic damage. The defects that arise are divided into point, line, surface, and volume defects depending upon their dimensionality.<sup>[54]</sup>

Point defects occur if atoms are missing or placed at irregular sites. In real single crystals a series of such defects can occur, and can be due to silicon itself, or to foreign atoms. In the first case the point defects are said to be intrinsic, and in the second case, extrinsic. An intrinsic point defect can be either a vacancy ( $V_{Si}$ ) at a normal Si site, or a matrix atom at an interstitial site between regular Si sites. An extrinsic point defect is produced by an atom of another element substituting a silicon atom at a normal lattice site, or by occupying an interstitial site. The controlled introduction of foreign atoms into regular sites by doping silicon (e.g., n-type doping with P or p-type doping with B at doping levels of between  $10^{17}$  and  $10^{20}$  atoms  $cm^{-3}$ ) is what makes the multifarious functionality of microchips possible.

The number of intrinsic point defects in silicon depends upon the temperature and the growth conditions of the CZ growth. At between 700 and 1200 °C there may be  $10^{15}$  to  $10^{17} cm^{-3}$  vacancies in CZ Si single crystals.<sup>[55]</sup> Occupation of the interstitial sites occurs somewhat less extensively. It is interesting to note that just one type of intrinsic point defect predominates within certain regions of CZ Si single crystals. Voronkov has shown that the occurrence of these point defects is dependent upon the relationship between the growth rate  $v$  and the axial temperature gradient  $G$  at the melt–crystal interface (the  $v/G$  rule).<sup>[56]</sup> Above a critical value  $(v/G)_{crit} \approx 0.13 mm^2 K^{-1} min^{-1}$ ,<sup>[31,57]</sup> intrinsic point defects will only survive as vacancies; below this value, they only occur at interstitial sites. For  $(v/G) > 0.13 mm^2 K^{-1} min^{-1}$ , the majority of vacancies are initially formed on drawing from the melt, whilst “interstitial atoms” are present to a lesser extent. Recombination of the deficient number of interstitial atoms with vacancies leads eventually to their complete disappearance. For  $(v/G) < 0.13 mm^2 K^{-1} min^{-1}$ , this mechanism is reversed. Most of the CZ Si single crystals produced industrially are manufactured under conditions in which Si vacancies are formed.<sup>[58]</sup>

During cooling the Si vacancies can coalesce to form agglomerates (voids, D defects).<sup>[59]</sup> The agglomeration of point defects during cooling can increase the dimensionality of the defects. In this way, one-dimensional line defects (dislocations) are formed. These are also formed during crystallization when mismatched crystal domains occur in the crystal due to mechanical strain, high temperature gradients,

or plastic deformation. Dislocations compensate such mismatches and can then extend across large regions of a single crystal. This can mean that half of a 300-mm diameter single crystal of about 2 m in length (Figure 5) is ruined<sup>[33]</sup> if dislocations subsequently spread into an originally displacement-free region with lengths that correspond approximately to the crystal diameter. Considerable economic damage is then accrued, since the growth of a large single crystal is a high-cost process that lasts several days. However, with the correct process control and the use of high-quality silica crucibles, such dislocations do not occur as the rapid crystallization of a thin, orientated Si seed leads to a neck being formed (“necking”; Figure 7d) so that further dislocations in the [100] direction can no longer occur. Through this process, a large single crystal of dislocation-free silicon (“DF-Si”) is obtained on drawing from the melt.<sup>[32]</sup>

On cooling the defects in the Si single crystal are subjected to strong dynamic forces, which must be controlled experimentally to ensure successful growth. Disklike accumulations of vacancies and additional Si atoms at interstitial sites can coalesce to form “dislocation loops” with enclosed stacking defects, which can involve either a deficiency or an excess of silicon atoms. In a two-dimensional representation lines are formed, however, in the real three-dimensional crystal, rings or loops with a radius of 10–15 lattice constants can form.<sup>[60]</sup> When the drawn CZ Si single crystal is cooled, dislocations can also “climb” up the lattice through interactions with point defects, as shown in Figure 14, where dislocations are marked by the dislocation symbol  $\perp$ , which symbolizes the start of the insertion of additional sites.

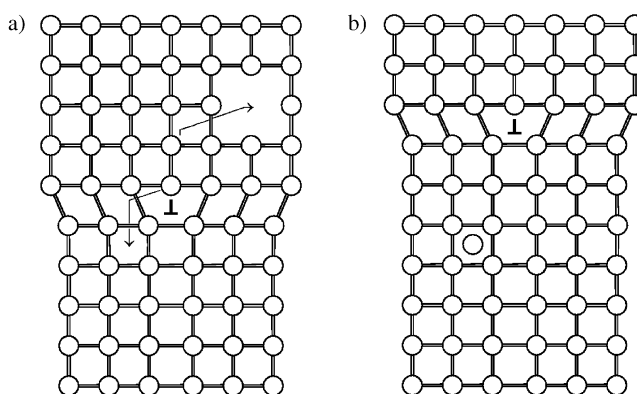


**Figure 14.** Schematic representation of the positive climbing of a dislocation in a two-dimensional lattice: a) the two arrows show the migration of the two neighboring atoms necessary for the climbing of the dislocation. b) After climbing an “interstitial site” is produced (emission) and an empty site is occupied (absorption). Explanation in text.

Of the two atoms labeled with arrows in Figure 14a, the lower becomes an interstitial atom (emission; Figure 14b), whereas the upper occupies a vacancy (absorption). In this way the step displacement climbs two horizontal rows vertically (positive climbing).<sup>[60]</sup> Negative climbing would occur during the emission of a vacancy and the absorption of an interstitial site.<sup>[60]</sup>

Intrinsic defects are able not only to react with other intrinsic defects, but also with extrinsic defects, that is, with foreign atoms which are present in low concentration within the single crystal. Oxygen is the most important impurity atom, and is thus the focus of numerous research projects. In spite of this a number of properties remain unexplained to this day and are thus still the subject of discussion.<sup>[55,61]</sup> Through their production in SiO<sub>2</sub> crucibles, industrially prepared CZ Si single crystals contain on the order of 10 ppma oxygen atoms, which corresponds to  $N_O = 5 \times 10^{17} \text{ cm}^{-3}$ . The interstitial oxygen atoms (O<sub>i</sub>) present in solid solution are electronically neutral and occupy sites between two silicon atoms.<sup>[55,61]</sup> For decades it was firmly believed that the Si-O<sub>i</sub>-Si arrangement in CZ silicon was angular (bond angle = 160°),<sup>[55,61]</sup> that is, similar to  $\alpha$ -quartz (144°).<sup>[62]</sup> The Si-O<sub>i</sub> bond length in CZ silicon at 1.60 Å should be almost as long as that in  $\alpha$ -quartz (1.61 Å).<sup>[62]</sup> More recently, a linear Si-O<sub>i</sub>-Si arrangement with a Si-O<sub>i</sub> bond length of 1.61 Å has also been discussed.<sup>[63]</sup> This Si-O<sub>i</sub>-Si configuration would arise when the energy threshold between the six possible angular configurations in the [111] direction and the linear version is only a few meV,<sup>[63]</sup> so that the O<sub>i</sub> atoms are able to move through the Si-Si matrix and are delocalized to a small degree.<sup>[64]</sup>

Figure 15 displays the silicon-rich part of the Si-O phase diagram.<sup>[65]</sup> Above 1414 °C (the melting point of silicon<sup>[30,31]</sup>) the O<sub>i</sub> atoms are found in liquid solution (L<sub>1</sub>, monophasic) up

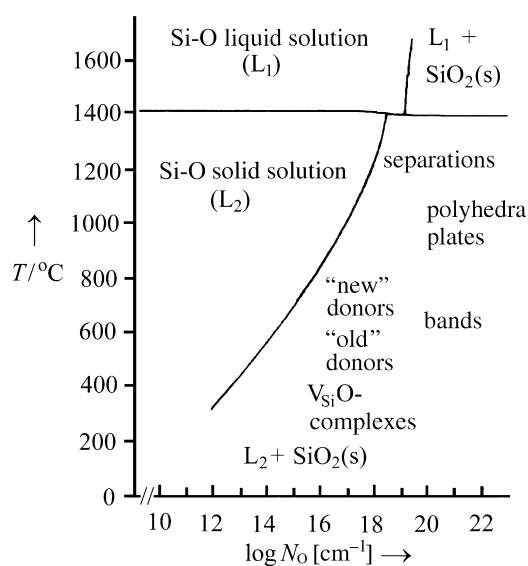


**Figure 15.** Silicon-rich section of the Si-O phase diagram. Data after Ref. [65].

to  $N_O \approx 10^{19} \text{ cm}^{-3}$ . An increase in  $N_O$  by a factor of 10 leads to segregation of solid SiO<sub>2</sub> in the melt (L<sub>1</sub> + SiO<sub>2</sub>(s), biphasic). On cooling to just below 1414 °C the solid Si-O solution is stable only to  $N_O = 2 \times 10^{18} \text{ cm}^{-3}$  (Figure 15), which corresponds to 0.004 at% oxygen (40 ppma). With falling temperature the oxygen solubility in solid silicon falls further: at 1100 °C  $N_O$  is only  $3 \times 10^{17} \text{ cm}^{-3}$  (0.0006 at%; 6 ppma), and at

1000 °C it is merely  $1 \times 10^{17} \text{ cm}^{-3}$  (0.0002 at%; 2 ppma). A CZ Si single crystal which at its melting point contains homogeneously dissolved oxygen at a concentration of about 10 ppma is supersaturated with oxygen on cooling to 1000 °C. According to the solubility curve only a fraction ( $\approx 2$  ppma) remains homogeneously dissolved in the silicon (homogeneously solid Si-O phase, L<sub>2</sub>), whilst the main fraction ( $\approx 8$  ppma) separates as a solid SiO<sub>x</sub> phase in the heterogeneous mixture L<sub>2</sub> + SiO<sub>2</sub>(s). The separation of solid SiO<sub>x</sub> phases continues with further cooling. A number of SiO<sub>x</sub> phases for an oxygen concentration of about  $N_O = 10^{20} \text{ cm}^{-3}$  are shown in the phase diagram (Figure 15; for example, separations, polyhedra, plates, bands, thermal donors, vacancy-oxygen complexes (V<sub>Si</sub>O complexes)). This complicated behavior is indicative of the ability of silicon and oxygen to form modified Si-O bonds, the structural variety of which is also shown in SiO<sub>2</sub> modifications.

On further cooling between 1400 and 700 °C, the CZ Si single crystal may exhibit smaller separations of amorphous SiO<sub>2</sub> at dislocation rings. These separations may coalesce to give somewhat larger agglomerates due to the lowering of interfacial energy through Ostwald ripening.<sup>[66]</sup> The agglomerates produce new dislocations in order to reduce mechanical stress arising from the local volume increase during SiO<sub>2</sub> separation. According to thermal studies, and as is characterized by the diffusion kinetics highlighted in Figure 15, the separations can also form polyhedra, plates, or bands. At higher temperatures (above 950 °C) polyhedra of minimal surface energy are formed. The preferred polyhedron is the octahedron because for silicon the surface energy is here lower than for a sphere.<sup>[67]</sup> At moderate temperatures (950–650 °C) plates can separate by reaction with dislocations, and needles can form at low temperatures (650–400 °C).<sup>[67]</sup>

An oxygen concentration of about  $N_O = 10^{20} \text{ cm}^{-3}$  (Figure 15) is sufficient to allow imagery of the SiO<sub>x</sub> separations obtained between 700 and 1400 °C with transmission electron microscopy (TEM), but these defects are electronically inactive. In contrast, by tempering the single crystals at lower temperatures (350–550 °C)<sup>[67]</sup> and by using a lower oxygen concentration ( $N_O \approx 10^{18} \text{ cm}^{-3}$ ) defects are obtained that are electrically active; these defects are known as thermal donors (TDs).<sup>[67]</sup> TDs are detectable through electrical resistance, infrared absorption, electron paramagnetic resonance (EPR), and electron-nucleus double resonance (ENDOR) spectroscopy, but are not observed in TEM because of their small size and the low oxygen concentration.<sup>[67]</sup>

TDs were initially divided into two groups with the poorly characteristic definitions “old” and “new” (Figure 15). In thermal donors electrons occupy states near the conduction band. There are, therefore, more appropriate names that characterize the electrical properties of the “old” thermal donors: single thermal donors are known as “shallow thermal donors” (STDs) and double thermal donors are called “thermal double donors” (TDDs).<sup>[68]</sup> The STDs are located in the electronic band structure of silicon at 0.035 eV<sup>[69]</sup> an ionization energy close to that of n-type P-doped silicon (0.044 eV),<sup>[70]</sup> and lying near to the minimum of the con-



duction band (hence, a shallow donor), whereas double donors with ionization energies of 0.053–0.155 eV.<sup>[68]</sup> are more distant. The TDDs are thought to consist of  $O_{mi}$  clusters with  $n = 2$ –13 oxygen atoms inserted between the silicon atoms in either chain or ring-shaped configurations.<sup>[61,68,71]</sup> The slow formation of the first thermal donors  $O_{mi}$  ( $n = 2$ ), to which further  $O_i$  atoms attach themselves, is the rate-determining step in the formation of higher members of the  $O_{mi}$  series.<sup>[61,71]</sup> Seventeen different TDDs are thought to occur.<sup>[68]</sup> Since thermal donors affect the conductivity of the CZ Si wafers they are of considerable significance in microprocessor technology.

Optimization of the technical processes that lead to oxygen aggregation in CZ Si single crystals will remain dependent upon empirical knowledge, so long as attempts to understand the complete atomic mechanism remain unsuccessful. Thus oxygen atoms triply coordinated with silicon atoms, and formally positively charged ions are responsible for the electrical activity of the thermal donors.<sup>[68]</sup> Density functional theory calculations on simple defects in CZ silicon have proved to be very helpful in estimating energies for the migration, restructuring, and dissociation of oxygen defects (e.g.,  $O_{mi}$  with  $n = 3$ –6) along a reaction coordinate.<sup>[72]</sup> Figure 16 illustrates some concepts for five simple oxygen defects:<sup>[68,73]</sup> Figure 16a shows the interstitial oxygen atom  $O_i$  in the angular configuration,<sup>[73]</sup> Figure 16b displays the interstitial oxygen dimer  $O_{2i}$  in the staggered configuration,<sup>[73]</sup>

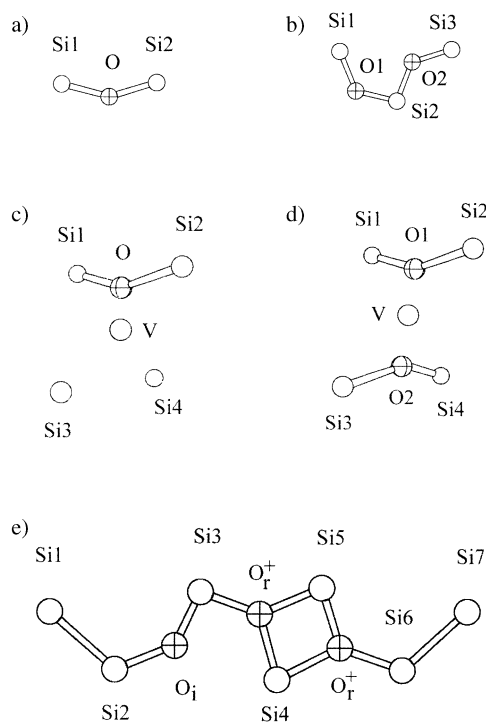


**Figure 16.** The arrangement of five possible oxygen defects in CZ silicon single crystals, as obtained by density functional theory (using the LDA approximation).<sup>[68,73]</sup> a) An interstitial oxygen atom  $O_i$  in the angular configuration, b) an interstitial oxygen dimer  $O_{2i}$  in the staggered configuration, c) a 1:1 vacancy–oxygen defect  $V_{Si}O$ , d) a 1:2 vacancy–oxygen defect  $V_{Si}O_2$ , e) thermal double donor  $O_i-O_{2r}^{2+}$ .

Figure 16c and d show the 1:1 and 1:2 vacancy–oxygen defects  $V_{Si}O$  and  $V_{Si}O_2$ ,<sup>[73]</sup> and Figure 16e describes the TDD  $O_i-O_{2r}^{2+}$ .<sup>[68]</sup> The Si–O–Si bond angles of approximately 140–160° and the Si–O bond lengths of approximately 1.62–1.65 Å are assigned as the  $O_i$ ,  $O_{2i}$ ,  $V_{Si}O$  and  $V_{Si}O_2$  defects (Figure 16a–d).<sup>[73]</sup> Thus the interactions lie in the range that has also been found experimentally for  $\alpha$ -quartz.<sup>[62]</sup> The doubly bound  $O_i$  atom in the TDD  $O_i-O_{2r}^{2+}$  (Figure 16e) is also coordinated in a manner similar to that in  $\alpha$ -quartz, whereas for the two triply bonded, formally positively charged  $O_r^+$  ring atoms, pyramidal or planar configurations are possible. Molecular-dynamics calculations on oxygen atoms triply coordinated with silicon predict Si–O bond lengths of 1.81 Å ( $2\times$ ) and 1.90 Å<sup>[74]</sup> and angles in the region of 120°.<sup>[75]</sup>

Electrically inactive oxygen agglomerates (with oxygen concentrations higher than those of the thermal donors; Figure 15) are in part advantageous because they render harmless the rapidly diffusing transition-metal impurities such as Fe, Cu, and Ni, which can interfere many microchip applications at concentrations as low as  $10^{11}$  atoms  $\text{cm}^{-3}$ .<sup>[76]</sup> For silicon with  $5 \times 10^{22}$  Si atoms per  $\text{cm}^3$ , this corresponds to an Fe content of  $2 \times 10^{-10}$  at %, or 2 ppta (1 ppt =  $10^{-3}$  ppb =  $10^{-6}$  ppm). The transition-metal impurities reduce the lifetime of the minority carriers through the recombination of corresponding electron hole pairs. Therefore it is advantageous to capture them along with oxygen agglomerates in an “internal gettering” (IG) process.<sup>[77]</sup>

In thin silicon wafers a two-hour tempering process at 1100°C precedes the IG process in a three-stage cycle. Through this procedure the internal oxygen concentration is greatly reduced since oxygen atoms diffuse out to the surface of the wafer, forming a low-defect surface or denuded zone (DZ).<sup>[78]</sup> Finally the wafer is cooled to 600°C for 4 h so that a large number of microdefect nuclei are formed at which  $\text{SiO}_x$  separations are established through heating for 12 h at 1100°C. This process is of considerable importance in the manufacture of microprocessors, as two objectives are achieved, namely, the preparation of a low-defect surface zone and a region inside the wafer in which the damaging transition-metal impurities Fe, Cu, and Ni are captured by IG.

It is evident that very careful thermal processing of the CZ Si single crystal drawn from the melt, and of the wafer that is then produced, is necessary to control the numerous defect reactions (defect engineering) that are possible.<sup>[79]</sup> Crystal drawing and defect engineering represent two equally strong but mutually dependent pillars which underpin 300-mm silicon technology. With an increasing diameter of the silicon single crystal and, in addition, ever diminishing cross-link structures in microchips, it is necessary continually to improve the construction of the crystals.<sup>[33]</sup> These improvements will become more difficult because CZ Si single crystals with increasing diameters must be produced with a respectively lower drawing rate, and for economic reasons greater crucible batch weights will have to be used. The residence time of the Si melt in the  $\text{SiO}_2$  crucible is then correspondingly increased. This demands continually better crucible qualities and more rigorous process control. Consequently the oxygen contamination of future CZ Si single crystals with large diameters will become problematic, and with it the defect engineering.

## 5. Summary and Outlook

In the CZ process large silicon single crystals are drawn and processed into wafers, the new generation of which (since December 2001) have a diameter of 300 mm. Production strategies estimate<sup>[2]</sup> that in 2009 the diameter will have increased to 450 mm, and in 2015 (99 years after Czochralski's discovery<sup>[5]</sup>) perhaps as large as 675 mm. With these predicted leaps in innovation, the wafer area will double in size in each instance. It would appear that along with the findings of G. E. Moore<sup>[1]</sup> (namely, doubling the capacity of the electronic components within just two years with a concomitant halving in price), a further criterion is included, that is, further perfecting of the single crystal!

Today, however, 170 one-gigabit microchips can be produced from a 300-mm wafer, compared to only 70 64-megabit chips per 200-mm wafer. The enormous value of these developments must continue to be backed up by considerable industrial investment, developments which, let us not forget, originated from Jan Czochralski's creative mistake!

*The authors extend their thanks to Dr. P. E. Tomaszewski (Polish Academy of Sciences) for the photographs of J. Czochralski and for his critical review of Sections 2 and 3, D. Schreiber (S. Fischer Verlag) for the photograph of W. Rathenau, Dr. C. Maywald-Pitellos (Gutenberg Museum, Mainz) for authentication of the photograph of W. Rathenau, Dr. J. Lexow (Bundesanstalt für Materialforschung und -prüfung) for the photograph of von Moellendorff, Dr. B. Altekürger (Crystal Growing Systems GmbH) for the photographs of the EKZ 3000/400 crystal drawing plant and for information on the publication of 300-mm silicon single-crystal technology, Dr. M. Kämper for his stimulating assistance, and last, but not least, R. Singer-Schülmers for her untiring dedication to this manuscript.*

Received: February 18, 2003 [A587]

- [1] Moore's Law: G. E. Moore, *Electronics* **1965**, 38, 114–117.
- [2] A. P. Mozer, *Mater. Sci. Eng. B* **2000**, 73, 36–41.
- [3] Infineon Technologies AG (München), press release (December 12, 2001), *Pioneering 300*. <http://www.pioneering300.com/pioneering300/de/>
- [4] W. Zulehner, *Mater. Sci. Eng. B* **2000**, 73, 7–15.
- [5] J. Czochralski, *Z. Phys. Chem. (München)* **1918**, 92, 219–221.
- [6] *Wielka Encyklopedia Powszechna PWN*, supplement, Państwowe Wydawnictwo Naukowe, Warszawa, **1970**, p. 99.
- [7] P. E. Tomaszewski, *Wiad. Chem.* **1987**, 41, 597–634.
- [8] J. Żmija, *Zesz. Nauk. – Politech. Łódz. Fiz.* **1989**, 10, 7–22 (Conf. Cryst. Growth Liq. Cryst. 1986).
- [9] P. E. Tomaszewski, *American Association for Crystal Growth*, Vol. 27(2), newsletter, **1998**, p. 12–18. <http://www.ptwk.org.pl/art2.htm> Dr. P. E. Tomaszewski, Institute of Low Temperature and Structure Research, Polish Academy of Sciences, P. Nr. 1410, 50–950 Wrocław 2, Poland.
- [10] P. E. Tomaszewski, *J. Cryst. Growth* **2002**, 236, 1–4.
- [11] P. Tomaszewski, *Jan Czochralski i jego metoda – Jan Czochralski and his Method*, Instytut Niskich Temperatur i Badań Strukturalnych PAN (Institute of Low Temperature and Structure Research), Polish Academy of Sciences, Wrocław, Poland.
- [12] Biography: *Wichard von Moellendorff*, 1881–1937; Deutsches Historisches Museum (Berlin); *Lebendiges Virtuelles Museum Online (LeMo)*. <http://www.dhm.de/lemo/html/biografien/MoellendorffWichard/>
- [13] W. von Moellendorff, *Elektrotech. Maschinenbau* **1913**, 31, 242–244. Lecture: “Über das Kabelwerk Oberspree”, February 4, **1913**, Vienna.
- [14] K. Braun, *Konservatismus und Gemeinwirtschaft. Eine Studie über Wichard von Moellendorff*, Walter Braun, Duisburg, **1978**.
- [15] W. Ruske, G. W. Becker, H. Czichos, *125 Jahre Forschung und Entwicklung, Prüfung, Analyse, Zulassung, Beratung und Information in Chemie- und Materialtechnik*, Bundesanstalt für Materialforschung und -prüfung (BAM), Berlin, Wirtschaftsverlag NW, Verlag für neue Wissenschaft GmbH, Bremerhaven, **1996**, p. 133.
- [16] W. von Moellendorff, *Giesserei-Ztg.* **1914**, 11, 506–509 and 521–525.
- [17] W. von Moellendorff, J. Czochralski, *Z. Ver. Dtsch. Ing.* **1913**, 57, 931–935 and 1014–1020.
- [18] J. Czochralski, *Z. Metallkd.* **1925**, 17, 1–11.
- [19] Biography: *Walther Rathenau*, 1867–1922; Deutsches Historisches Museum (Berlin); *Lebendiges Virtuelles Museum Online (LeMo)*. <http://www.dhm.de/lemo/html/biografien/Rathenau-Walther/>
- [20] “*Walther Rathenau. Sein Leben und sein Werk*”: H. Kessler, *Gesammelte Schriften in drei Bänden, Vol. 3* (Eds.: C. Blasberg, G. Schuster), Fischer Taschenbuch, Frankfurt am Main, **1988**.
- [21] According to information from the ink-well specialist, Dr. C. Maywald-Pitellos (Gutenberg Museum, Mainz), it is an ink well with “a drop-shaped glass body... with a metal ring. Probably a cover, not seen in the photograph, belongs to the ink well. Ink wells with this shape could be obtained from department stores up until the Second World War.”
- [22] *Claims Resolution Tribunal*, Zürich, CRT-II, **2001** Published List of Accounts. [http://www.crt-ii.org/\\_lists/publication\\_list1\\_C.phtm](http://www.crt-ii.org/_lists/publication_list1_C.phtm)
- [23] J. Czochralski, *Schweiz. Arch. Angew. Wiss. Tech.* **1940**, 167–176.
- [24] J. Czochralski, *Moderne Metallkunde in Theorie und Praxis*, Springer, Berlin, **1924**.
- [25] Polish Physical Society, ul. Hoża 69, 00–681, Warsaw, Poland. <http://ptf.fuw.edu.pl/ptftabp.htm>
- [26] Polish Society for Crystal Growth, Institute of Technology of Electronic Materials, ul. Wólczyńska 133, 01–919 Warszawa, Poland. <http://www.ptwk.org.pl/cz-symposium03/index/html>
- [27] J. Czochralski, *Z. Ver. Dtsch. Ing.* **1917**, 16, 345–351.
- [28] Business, Concentrates, *Chem. Eng. News* **2002**, 80(42), 19.
- [29] B. Altekürger, M. Gier, *Vak. Forsch. Prax.* **1999**, 31–36.
- [30] According to Ref. [31], the precise melting point of silicon is very difficult to measure because thermoelements based on metals of the platinum group age readily in the region of 1400°C and can thus indicate temperatures up to 3°C too low. In addition the chemically aggressive silicon melt dissolves most impurities, with a concomitant drop in melting point. Since 1958, 20 melting points have been published: 1408, 1410, 1412(7×), 1414(8×), and 1416(3×)°C. That gives a mean value of 1413.1°C with a standard deviation of the mean of ±0.31°C. A temperature of 1414.0 ± 0.9°C is recommended as the melting point for silicon; this value is slightly higher than the mean value and should have a statistical reliability of 90%.
- [31] “Properties of Crystalline Silicon”: *Electronic Materials Information Service: EMIS Datareviews Series, Vol. 20* (Ed.: Robert Hull), INSPEC, The Institution of Electrical Engineers, London, **1999**.
- [32] W. Dash, *J. Appl. Phys.* **1959**, 30, 459–474.
- [33] “Festkörperprobleme”: A. P. Mozer, *Adv. Solid State Phys.* **1998**, 37, 1–14.

- [34] E. Tomzig, W. von Ammon, E. Dornberger, U. Lambert, W. Zulehner, *Microelectron. Eng.* **1999**, *45*, 113–125.
- [35] Crystal-drawing plant EKZ 3000/400 of CGS-Crystal Growing Systems GmbH, Hanau; crucible diameter: 1.02 m, charge weight: 600 kg, crystal movement: 4 m, furnace chamber diameter: 1.7 m, total height: 14.74 m.
- [36] T. Zhang, G.-X. Wang, H. Zhang, F. Ladeinde, V. Prasad, *J. Cryst. Growth* **1999**, *198/199*, 141–146.
- [37] “Elemente, anorganische Verbindungen und Materialien, Minerale”: *D'Ans-Lax, Taschenbuch für Chemiker und Physiker*, Vol. III, 4th revised edition (Ed.: R. Blachnik), Springer, Berlin, **1998**, p. 193.
- [38] G. Müller, A. Mühe, R. Backofen, E. Tomzig, W. von Ammon, *Microelectron. Eng.* **1999**, *45*, 135–147.
- [39] Y. C. Won, K. Kakimoto, H. Ozoe, *J. Cryst. Growth* **2001**, *233*, 622–630.
- [40] R. W. Series, D. T. J. Hurle, *J. Cryst. Growth* **1991**, *113*, 305–328.
- [41] W. H. Westphal, *Physik: Ein Lehrbuch*, Springer, Berlin, **1959**, p. 370.
- [42] M. Petschenig, *Der kleine Stowasser*, Lateinisch-Deutsches Schulwörterbuch, G. Freytag, München, **1963**, p. 150.
- [43] *The New Encyclopaedia Britannica*, Vol. 3, *Micropaedia*, Encyclopaedia Britannica, Chicago, **1997**, p. 810.
- [44] *Langenscheidts Fachwörterbuch Technik und angewandte Wissenschaften*, English-German (Ed.: P. A. Schmitt), Langenscheidt, Berlin, **2002**, p. 466.
- [45] D. Vizman, J. Friedrich, G. Müller, *J. Cryst. Growth* **2001**, *230*, 73–80.
- [46] H. Yamagishi, M. Kuramoto, Y. Shiraishi, N. Machida, K. Takano, N. Takase, T. Iida, J. Matsubara, H. Minami, M. Imai, K. Takada, *Microelectron. Eng.* **1999**, *45*, 101–111.
- [47] Data according to Ref. [39]: coil separation: 750 mm; distance from the coils to the melt surface: 230 mm; crucible diameter: 75 mm; crucible height: 37.5 mm; crystal diameter: 37.5 mm;  $\omega_{\text{crystal}} = -3$  revolutions per minute ( $\text{rmin}^{-1}$ ),  $\omega_{\text{crucible}} = 10 \text{ rmin}^{-1}$ ; The Hartmann number  $Ha$  is dimensionless. It is defined as  $Ha = Bh(\sigma\mu^{-1})^{1/2}$ , with  $B$  is the magnetic field strength,  $H$  is the height,  $\sigma$  is the electrical conductivity, and  $\mu$  is the viscosity.<sup>[48]</sup> According to a private communication from H. Ozoe the calculations are first carried out with a dimensionless mathematical model in order to obtain results independent of specific parameters. Therefore in the original figure (Figure 2 in Ref. [39]) the oxygen concentration (atoms per  $\text{cm}^3$ ) is shown on the ordinate and the dimensionless time on the abscissa. Multiplication of this time by the factor  $t_0 = 0.0123 \text{ s}$  (Table 1 in Ref. [39]), which is appropriate for the above model, gives  $t$  [s] for the abscissa of Figure 12.
- [48] *dtv-Lexikon der Physik*, Vol. 4 *Glu-Kel* (Ed.: H. Franke), Deutscher Taschenbuch Verlag, München, **1970**, p. 81.
- [49] “Modelling of Transport Phenomena in Crystal Growth”: K. Kakimoto, *Developments in Heat Transfer*, Vol. 6 (Ed.: J. S. Szmyd), WIT Press, Southampton, **2000**, p. 181–200.
- [50] A. Seidl, G. McCord, G. Müller, H.-J. Leister, *J. Cryst. Growth* **1994**, *137*, 326–334.
- [51] The isothermal lines<sup>[45]</sup>  $(T - T_m)(T_{\text{max}} - T_m)^{-1}$  of Figure 12 were converted into temperatures  $T$  in °C for  $T_m = 1414^\circ\text{C}$  (melting point of  $\text{Si}^{[30,31]}$ ) and  $\Delta T_{\text{max}} = 36^\circ\text{C}$  and  $42^\circ\text{C}^{[45]}$  respectively, and are inserted on the right of the figure.
- [52] M. Kurz, A. Pusztai, G. Müller, *J. Cryst. Growth* **1999**, *198/199*, 101–106.
- [53] N. Van den Bogaert, F. Dupret, *J. Cryst. Growth* **1997**, *171*, 65–76 und 77–93.
- [54] W. Kleber, *Einführung in die Kristallographie*, extended and revised by H. J. Bautsch, J. Bohm, I. Kleber, 15th Edition, VEB Verlag Technik, Berlin, **1983**, p. 164.
- [55] S. Pizzini, *Solid State Phenom.* **2002**, *85–86*, 1–66.
- [56] V. V. Voronkov, *J. Cryst. Growth* **1982**, *59*, 625–643.
- [57] W. von Ammon, E. Dornberger, H. Oelkrug, H. Weidner, *J. Cryst. Growth* **1995**, *151*, 273–277.
- [58] R. Falster, V. V. Voronkov, *Mater. Sci. Eng. B* **2000**, *73*, 87–94.
- [59] V. V. Voronkov, R. Falster, *J. Cryst. Growth* **1999**, *204*, 462–474.
- [60] J. Bohm, *Realstruktur von Kristallen*, E. Schweizerbart'sche Verlagsbuchhandlung (Nägele and Obermiller), Stuttgart, **1995**, p. 126 and 162.
- [61] R. C. Newman, *J. Phys. Condens. Matter* **2000**, *12*, R335–R365.
- [62] A. F. Wells, *Structural Inorganic Chemistry*, Clarendon Press, Oxford, **1984**, p. 1006.
- [63] J. Coutinho, R. Jones, P. R. Briddon, S. Öberg, *Phys. Rev. B* **2000**, *62*, 10824–10840.
- [64] E. Artacho, F. Ynduráin, B. Pajot, R. R. Ramírez, C. P. Herrero, L. I. Khiruenko, K. M. Ito, E. E. Haller, *Phys. Rev. B* **1997**, *56*, 3820–3833.
- [65] J. C. Mikkelsen, *Mater. Res. Soc. Symp. Proc.*, **1986**, *59*, 3–5 and 19–30.
- [66] W. Ostwald, *Z. Phys. Chem. (München)* **1900**, *34*, 495–503.
- [67] A. Borghesi, B. Pivac, A. Sassella, A. Stella, *Appl. Phys. Rev.* **1995**, *77*, 4169–4244.
- [68] M. Pesola, Y. J. Lee, J. von Boehm, M. Kaukonen, R. M. Nieminen, *Phys. Rev. Lett.* **2000**, *84*, 5343–5346.
- [69] J. A. Griffin, H. Navarro, J. Weber, L. Genzel, J. T. Borenstein, J. W. Corbett, L. C. Snyder, *J. Phys. C* **1986**, *19*, L579–L584.
- [70] G. Busch, H. Schade, *Vorlesungen über Festkörperphysik*, Birkhäuser, Basel, **1973**, p. 299.
- [71] R. C. Newman, *Mater. Sci. Eng. B* **1996**, *36*, 1–12.
- [72] Y. J. Lee, J. von Boehm, M. Pesola, R. M. Nieminen, *Phys. Rev. B* **2002**, *65*, 085205-1–085205-12.
- [73] M. Pesola, J. von Boehm, T. Mattila, R. M. Nieminen, *Phys. Rev. B* **1999**, *60*, 11 449–11 463.
- [74] A. Pasquarello, *Appl. Surf. Sci.* **2000**, *166*, 451–454.
- [75] A. Pasquarello, M. S. Hybertsen, R. Car, *Nature* **1998**, *396*, 58–60.
- [76] M. L. Polignano, F. Cazzaniga, A. Sabbadini, F. Zanderigo, F. Priolo, *Mater. Sci. Semicond. Process.* **1998**, *1*, 119–130.
- [77] F. Shimura, *Solid State Phenom.* **1991**, *19–20*, 1–12.
- [78] K. Nagasawa, Y. Matsushita, S. Kishino, *Appl. Phys. Lett.* **1980**, *37*, 622–624.
- [79] T. Sinno, E. Dornberger, W. von Ammon, R. A. Brown, F. Dupret, *Mater. Sci. Eng. R* **2000**, *28*, 149–198.
- [80] Wichard von Moellendorff, executive engineer at the Allgemeinen Elektrizitäts-Gesellschaft (AEG), “On the Oberspree Cable Factory, with cinematographic presentation”; lecture given at 7 p.m. on February 4, 1913, in Vienna.<sup>[13]</sup>